RSC Advances

ROYAL SOCIETY OF CHEMISTRY

www.rsc.org/advances

Optically Temperature Sensing Property of Yb^{3+}-Er^{3+} Co-doped $NaLnTiO_4$ (Ln=Gd, Y) Up-conversion Phosphors

Dong He[a], Chongfeng Guo[a*], Sha Jiang[b], Niumiao Zhang[a], Changkui Duan[b*], Min Yin[b], Ting Li[a],

a. *National Key Laboratory of Photoelectric Technology and Functional Materials (Culture Base) in Shaanxi Province, National Photoelectric Technology and Functional Materials & Application of Science and Technology International Cooperation Base, Institute of Photonics & Photon-Technology, Northwest University, Xi'an, 710069, China;*

b. *School of Physical Science, University of Science and Technology of China, Hefei, 230026, China;*

----

* Author to whom correspondence should be addressed

Institute of Photonics & Photon-Technology;

Northwest University,

Xi'an 710069, China.

Tel. & Fax.: 86-29-88302661

E-mail: guocf@nwu.edu.cn (Prof. Guo)

Abstract

The Yb^{3+}/Er^{3+} ions co-doped $NaLnTiO_4$ (Ln = Y, Gd) up-conversion (UC) phosphors were successfully synthesized by sol-gel method. The phase purity and the structure of the samples were characterized by powder X-ray diffraction (XRD), and the optimal compositions were also determined according to their UC emission intensities. Samples emit orange light and their UC spectra were recorded with the excitation of a laser diode with 980 nm wavelength. UC luminescence intensity could be enhanced greatly after introducing sensitizer Yb^{3+} ions, and the energy transfer (ET) from Yb^{3+} to Er^{3+} plays a vital roles. The UC mechanism and processes responsible for the emissions were investigated to involve two-photon absorption. The lifetime of green emission in Er^{3+} singly doped and Yb^{3+}-Er^{3+} co-doped were measured to prove the existence of ET. The temperature dependence of fluorescence intensity ratios (FIR) for the two green UC emission bands peaked at 530 and 550 nm was studied in the range of 300-510 K under an excitation of 980 diode laser with about $4W/cm^2$ power density, and the maximum sensitivity was approximately 0.0045 K^{-1} at 510K for $NaYTiO_4$ and 480K for $NaGdTiO_4$, respectively. It indicates that Yb^{3+}/Er^{3+} ions co-doped $NaLnTiO_4$ (Ln = Y, Gd) phosphor is potential candidates for optical temperature sensors.

Keywords: Up-conversion; Energy transfer; Optically Temperature sensing; Er^{3+}.

1. Introduction

Temperature is a fundamental and significant physical parameter, which could be accurately measured by many methods. Conventional temperature measurements are based on the principle of liquid and metal expansion, which is realized by heat flow to an invasive probe. However, these contact methods could not be used in many cases, such as the electrical transformer in power stations, oil refineries and intracellular temperature, which promote the development of non-contract thermometry technique. Recently, the non-contract temperature sensing based on rare earth (RE) ions activated luminescent material *has* been given more attention [1-7]. In particular, the fluorescence intensity ratio (FIR) technique is regarded as the most promising, which *involves* the measurement of photoluminescence intensities from two thermally coupled energy levels

(TCLs) of RE ion. FIR technique could offer excellent measurement accuracy because it is independent of spectrum losses and fluctuations in the excitation intensity. Now, optical temperature sensors based on RE activated up-conversion (UC) phosphor have been extensively investigated [8-12]. Among these RE ions, Er^{3+} is the most popular activator because its two thermally coupled levels (TCLs) $^2H_{11/2}$ and $^4S_{3/2}$ and characteristic green UC emission from TCLs. However, only low luminescence efficiency is obtained in Er^{3+} solely doped phosphor under the 980 nm laser excitation due to the low absorption. The Er^{3+} and Yb^{3+} are usually used in couples, which could improve the luminescence efficiency of UC phosphor remarkably due to the high and broad absorption (ranging from 850-1050 nm) of Yb^{3+} and efficiently transfer its energy to Er^{3+} [13-17].

The layered perovskite titanates complex oxides $ALnTiO_4$ (A=Li, Na, K; Ln = rare earth) have been proven to serve as excellent phosphor hosts due to their typical two-dimensional *structures* and good chemical and physical *stabilities* [18-20]. They usually show higher critical concentration than those of other conventional inorganic phosphors because the energy transfer is restricted to quasi-two-dimensional sub-lattice in present compounds [21]. Recently, a series of Eu^{3+} doped red emitting phosphors $ALnTiO_4$ (A=Na, K; Ln = La, Gd, Y):Eu^{3+} have been prepared by sol-gel method in our group, results indicate that they show high luminescence *efficiencies* and could be used as red components in white light-emitting diodes (w-LEDs) and field emission displays (FEDs) [22-23]. However, *very little research* on UC phosphors using $ALnTiO_4$ (A=Li, Na, K; Ln = rare earth) as hosts has been carried out [24].

In this paper, UC phosphors based on Yb^{3+} and Er^{3+} doped $NaLnTiO_4$ (Ln=Y, Gd) were prepared by sol-gel method and their UC luminescence properties were investigated. The UC emission mechanisms were evaluated, and the energy transfer *processes* between Yb^{3+} and Er^{3+} were proved through the measurements of lifetime. Additionally, their thermometry behaviors have also been illustrated by FIR technique.

2. Experimental

2.1. Synthesis of samples

The Yb^{3+} sensitized Er^{3+} doped $NaLnTiO_4$ (Ln=Y, Gd) phosphors with composition

$NaLn_{1-x-y}Yb_xEr_yTiO_4$ were prepared using a modified sol-gel method. In present systems, Yb^{3+} and Er^{3+} ions are expected to occupy the sites of Ln^{3+} due to their identical valence and similar ionic radius. Here, the starting materials include analytical reagent (AR) Na_2CO_3, rare earth oxides Y_2O_3, Gd_2O_3, Yb_2O_3, Er_2O_3 with high purity (99.99%, ShanghaiYuelong Nonferrous Metals Ltd.) and analytical reagent tetrabutyl titanate $Ti(OC_4H_9)_4$, which are used as for the *sources* of Na, Y (or Gd), Yb, Er and Ti, respectively. In addition, anhydrous ethanol and acetic acid played the role of solvent and hydrolysis inhibitor in this experiment. According to the chemical formula of the UC phosphors $NaLn_{1-x-y}Yb_xEr_yTiO_4$: (a) x=0.1, y=0.01, 0.03, 0.05, 0.07, 0.09, and (b) y=0.05, x=0.06, 0.08, 0.10, 0.12, 0.14, 0.16, 0.18, 0.20, a stoichiometric amount of oxides Ln_2O_3（Ln=Y, Gd, Yb and Er）and Na_2CO_3 (excess 30% as flux) were first dissolved in dilute HNO_3(AR) under continuous stirring, and the excess HNO_3 was evaporated at high temperature. Then, the required amount of deionized water was added to get transparent solution A after fully stirring. The calculated volume of $Ti(OC_4H_9)_4$, ethanol and acetic acid were mixed to form the transparent solution B. Subsequently, solution B was transferred to solution A drop by drop under constant stirring to get the final transparent solution. The final transparent solution was kept at 70 ℃ for 24 h until an ivory white resin formed. The resin was further dried at 120 ℃ for 24 h to get a dried gel. The dried gel was ground and preheated in a furnace at 500 ℃ for 5 h, and then sintered at required temperature at 900 ℃ for 2 h to obtain final samples.

2.2 Characterization

The crystal structures were identified by powder X-ray diffractions (XRD) using a Rigaku-Dmax 3C powder diffractometer (Rigaku Corp, Tokyo, Japan) with Cu-Ka radiation (λ = 1.5406 Å). UC luminescence spectra of the phosphors at room temperature (RT) were recorded using a Hitachi F-4600 spectrophotometer (Hitachi high technologies corporation, Tokyo, Japan) with an external power-controllable 980 nm semiconductor laser (Hi-Tech Optoelectronics Company, Beijing, China) as excitation source. The lifetimes for $^4S_{3/2} \rightarrow {}^4I_{15/2}$ transitions of Er^{3+} at 547 nm at RT were carried out *using an 980 nm* optical parametric oscillator (OPO) *pulsed laser* as excitation source, and the signals were detected by a Tektronix digital oscilloscope (TDS 3052). In order to investigate the temperature dependence of the UC emission, the sample was placed in a temperature-controlled copper cylinder, and its temperature was increased from RT to 240 ℃. The UC spectra of sample at various temperatures were obtained using a Jobin-Yvon HRD-1 double monochromator equipped with a Hamamatsu R928 Photomultiplier under the excitation of a 980 nm diode laser with 164 mW and the excitation power density was about $4W/cm^2$. The signal was analyzed by an EG&G 7265 DSP Lock-in Amplifier and stored into computer memories.

3. Results and Discussion

3.1 Crystal structure and phase composition

The *structures* and *compositions* of the obtained products were characterized by XRD. Figure 1 shows the XRD patterns of $NaY_{1-x-y}Yb_xEr_yTiO_4$ and $NaGd_{0.81}Yb_{0.14}Er_{0.05}TiO_4$ phosphors. XRD patterns of $NaY_{0.90-y}Yb_{0.10}Er_yTiO_4$ and $NaY_{0.95-x}Yb_xEr_{0.05}TiO_4$ samples as a function of Er^{3+} concentrations y and Yb^{3+} concentrations x are shown in Fig. 1a, it *is* observed that all diffraction peaks of samples can readily be identified as the characteristic peaks of pure orthorhombic phase $NaYTiO_4$ with JCPDS standard card No. 50-0022. Results indicate that no noticeable diffraction peaks from *any* impurity phases are found within the whole range of our experiments, which illuminates that the parameters to synthesis of the present samples are fit. In addition, it is found that the positions of the strongest diffraction peak (113) gradually shift to high angle, which due to the smaller radius of Yb^{3+} (0.86Å) or Er^{3+} (0.88Å) ions than that of Y^{3+} (0.89Å) [25]. As a representative, XRD pattern of $NaGd_{0.81}Yb_{0.14}Er_{0.05}TiO_4$ phosphor is shown in Fig. 1b with the standard $NaGdTiO_4$ (JCPDS 86-0830) profile, all of their diffraction peaks are matched well. Above results *prove* that Yb^{3+} or Er^{3+} ions occupy the sites of Y^{3+} and do not alter the host structure significantly.

3.2 Effects of do-pant contents on Up-conversion emission

It is well known that the UC emission intensity greatly depends on the concentrations of the doped ions, thus we investigated the effect of dopant contents on $NaY_{1-x-y}Yb_xEr_yTiO_4$: xYb^{3+}, yEr^{3+} phosphors with the continue wave (CW) excitation at 980 nm. Room temperature UC spectra of samples as function of Er^{3+} and Yb^{3+} contents are displayed in Fig. 2a and b, respectively. The obtained emission spectra of Er^{3+}/Yb^{3+} codoped $NaYTiO_4$ UC phosphors consist of two green emission (530 and 550 nm) bands and a red emission (668 nm) band, which are assigned to ${}^2H_{11/2}\rightarrow{}^4I_{15/2}$, ${}^4S_{3/2}\rightarrow{}^4I_{15/2}$ and ${}^4F_{9/2}\rightarrow{}^4I_{15/2}$ the characteristic inner shell transitions of Er^{3+} from the excited levels to the ground state of $4f$ electronic configuration, respectively. The normalized integrated intensities for green (from 510 to 570 nm) and red (from 640 to 690 nm) UC emissions were also calculated and presented in the insets of Fig. 2*a* and *b* with variable Er^{3+} or Yb^{3+} concentrations for the two series of samples, respectively. *From the inset of Fig. 2(a), it is found* that the UC luminescence intensities *for* both the green and red emissions increase first with increasing Er^{3+} contents and then decrease with the continual increase of Er^{3+} concentration after reaching the maximum at $y = 0.05$ due to the concentration quenching, which is caused by non-radiative energy transfer and the cross relaxation between Er^{3+} [26]. Figure 2b shows the UC spectra of samples $NaY_{1\text{-}x\text{-}0.05}Yb_{x}Er_{0.05}TiO_4$: xYb^{3+}, $0.05Er^{3+}$ with invariable Er^{3+} concentration $y = 0.05$ and variable Yb^{3+} concentrations ranging from 0 to 0.20, which shows similar trend as Fig.2a. Seen from Fig.2b, it is observed that the UC emission of sample $NaY_{0.95}Er_{0.05}TiO_4$ without Yb^{3+} is too weak to be checked due the weak absorption of Er^{3+} for 980 nm laser, and increases remarkably with the growth of Yb^{3+} dosage due to the efficient energy transfer from Yb^{3+} to Er^{3+} for the larger absorption cross section of Yb^{3+} at 980 nm and excellent energy levels match between Yb^{3+} and Er^{3+} [27]. Results indicate that the optimal concentration of Yb^{3+} is $x = 0.14$, and the UC emission intensity descends gradually as the concentration of Yb^{3+} beyond 0.14. The main reasons for this may come from the energy back transfer (EBT) Er^{3+} ($^4S_{3/2}$) +Yb^{3+} ($^2F_{7/2}$) → Er^{3+} ($^4I_{13/2}$) + Yb^{3+} ($^2F_{5/2}$) [28-29]. The higher Yb^{3+}concentration, the higher ratio of EBT from Er^{3+} to Yb^{3+} to ET from Yb^{3+} to Er^{3+} [24].

3.3 Energy Scheme and Mechanism of UC emission

In order to better understand the possible UC processes and the mechanisms of the green and red emission in Yb^{3+}/Er^{3+} co-doped $NaLnTiO_4$ (Ln=Y, Gd) phosphors, the energy level diagram for Er^{3+} and Yb^{3+}, feasible excitation pathways, emission process and UC mechanisms are demonstrated in Fig. 3. The possible up-conversion populating processes of the Er^{3+} and Yb^{3+} co-doped samples under the excitation of 980 nm are shown in Fig.3a. As *drawn* in the schematic, the energy level $^2F_{5/2}$ of Yb^{3+} is close to that of $^4I_{11/2}$ of Er^{3+}, thus the energy transfer from Yb^{3+} to Er^{3+} is high efficient. Under the excitation of 980 nm LD, Yb^{3+} first absorbs an infrared photon from the ground state transition $^2F_{7/2}$ to the excited state $^2F_{5/2}$. The excitation wavelength (980 nm) is in resonance with the transition of $^2F_{7/2}$→$^2F_{5/2}$ of Yb^{3+} and thus easy to be absorbed by this ion. For the green emission, the *peaks* at 530 and 550 nm come from the excited states $^2H_{11/2}/^4S_{3/2}$ to ground state $^4I_{15/2}$ transitions of Er^{3+}, and the $^4S_{3/2}$ *level* could be populated by non-radiative (NR) relaxation from the upper $^2H_{11/2}$ *level* populated through NR process from $^4F_{7/2}$ *level* of Er^{3+}. The population $^4F_{7/2}$ *level* may follow three process: Er^{3+} ($^4I_{11/2}$) + a photon (980 nm) → Er^{3+} ($^4F_{7/2}$) (excited state absorption: ESA), Er^{3+} ($^4I_{11/2}$) + Yb^{3+} ($^2F_{5/2}$) → Er^{3+} ($^4F_{7/2}$) + Yb^{3+} ($^2F_{7/2}$) (energy transfer, ET),and Er^{3+} ($^4I_{11/2}$) + Er^{3+} ($^4I_{11/2}$) → Er^{3+} ($^4F_{7/2}$) + Er^{3+} ($^4I_{15/2}$) (cross relaxation: CR). Here, the intermediary level $^4I_{11/2}$ of Er^{3+} play an vital role in these processes, and population process of this energy includes the energy transfer (ET) process Er^{3+} ($^4I_{15/2}$) + Yb^{3+} ($^2F_{5/2}$) → Er^{3+} ($^4I_{11/2}$) + Yb^{3+} ($^2F_{7/2}$) and the ground state absorption (GSA) process from $^4I_{15/2}$ to $^4I_{11/2}$. However, the probability for the GSA of Er^{3+} is low due to the narrow absorption cross section, which illuminates that the ET process dominated the UC process [30]. For the red emission assigned to $^4F_{9/2}$→$^4I_{15/2}$ transitions of Er^{3+}, the population of $^4F_{9/2}$ could involve following these processes: Er^{3+}($^4I_{13/2}$) + a photon (980 nm) →Er^{3+}($^4F_{9/2}$) (ESA), Yb^{3+}($^2F_{5/2}$) + Er^{3+}($^4I_{13/2}$) →Yb^{3+}($^2F_{7/2}$) + Er^{3+}($^4F_{9/2}$) (ET), and the NR from $^4S_{3/2}$ to $^4F_{9/2}$. The long-lived intermediary $^4I_{13/2}$ level is populated by NR relaxation from $^4I_{11/2}$ level.

For a multi-photon UC process, the UC luminescence intensity (*I*, integrated intensity) depends on the *n*th the pump laser powder (*P*), *i. e.*, $I \propto P^n$, here *n* denotes the number of absorbed infrared (IR) photons to produce an UC emission photon [31] and it is important for the determination of UC mechanism. It is known that which could be assigned to the slope of the straight line that obtained through the plot of ln *I* versus ln *P.* Figure 3b and *c* shows the experimental data and fitting curves reflecting the relationship between the integrated UC intensities and pump power for the samples $NaY_{0.81}Yb_{.0.14}Er_{0.05}TiO_4$ and $NaGd_{0.81}Yb_{.0.14}Er_{0.05}TiO_4$ with optimal coposition, respectively. *As shown in* Fig. 3b and 3c, it could find that the slopes of the both curves for the green peak are 2.05 and 1.99 for Ln =Y and Gd, and the slopes are 1.87 and 1.83 for the red emission, *which are very close to 2.0 within the margin of error*. Results indicate that the green $^4S_{3/2}$→ $^4I_{15/2}$ and red $^4F_{9/2}$→$^4I_{15/2}$ transition in Yb^{3+}/Er^{3+} co-doped $NaLnTiO_4$ (Ln=Y, Gd) are two-photon absorption process.

3. 4 Lifetime measurements

According to above mentioned possible UC processes, the enhanced UC intensities with the addition of Yb^{3+} are attributed to the efficient energy transfer from Yb^{3+} to Er^{3+}, *and ET* plays a dominant role in this process. In order to prove the existance of the ET between Yb^{3+} and Er^{3+}, the emssion decay curves of the green ($^4S_{3/2}$→ $^4I_{15/2}$, 550 nm) for the samples $NaY_{0.95-x}Yb_xEr_{0.05}TiO_4$:

$0.05Er^{3+}$，xYb^{3+} (x = 0, 0.08.) with and without sensitizer Yb^{3+} were shown in Fig.4 after 980 nm pulsed laser excitation, in which the decay profiles of the $^4S_{3/2} \rightarrow ^4I_{15/2}$ (green) transitions are normalized. The lifetime could be calculated according to equation (1) [32]:

$$\tau = \frac{\int_0^\infty I(t)tdt}{\int_0^\infty I(t)dt} \tag{1}$$

where $I(t)$ is fluorescence intensity at time t. The decay curve can be well fitted with quadratic index equation, and the average lifetime can obtained through the following equation [33]:

$$\bar{\tau} = \frac{A_1 t_1{}^2 + A_2 t_2{}^2}{A_1 t_1 + A_2 t_2} \tag{2}$$

The corresponding lifetimes were listed in Fig.4, it could be found that the lifetime for Yb^{3+}-Er^{3+} co-doped $NaY_{0.87}Yb_{0.08}Er_{0.05}TiO_4$ is larger (84 μs) than that (36 μs) of Er^{3+} solely doped sample $NaY_{0.95}Er_{0.05}TiO_4$, which confirms the presence of ET from Yb^{3+} to Er^{3+} in present system.

3. 5 Temperature sensing properties

As already mentioned, UC bands centered at 530 and 550 nm arise from $^2H_{11/2} \rightarrow ^4I_{15/2}$ and $^4S_{3/2} \rightarrow ^4I_{15/2}$ transitions. The energy gap between the levels $^2H_{11/2}$ and $^4S_{3/2}$ of Er^{3+} is *around* 750 cm^{-1}, the state of $^2H_{11/2}$ may also be pupulated from $^4S_{3/2}$ by thermal excitation and the UC emission intensity ratio of emission band at 530 to 550 could change with the variable temperature, therefore it is could be used as optically temperature sensor for the present UC phosphors. In order to investigate the temperature sensing properties of synthesized *phosphors*, the green UC emission spectra for samples $NaLnTiO_4$: $0.05Er^{3+}$,$0.14Yb^{3+}$ (Ln = Y, Gd) at different temperature (from 300 to 510 *K*) were recored and displayed in Fig. 5a and b, in which the spectra are normalized to the most intense emission peak at about 551 nm. In present cases, the excitation power density was estimated to be around 4W/cm^2, which is low enough to neglect the heating effect from the pumping source. It is found that no remarkable *shift* in emission wavelength for two samples while their fluorescence intensity ratio (FIR) of UC emission from $^2H_{11/2} \rightarrow ^4I_{15/2}$ to $^4S_{3/2} \rightarrow ^4I_{15/2}$ (550 nm) increases with the rise of temperature. The relative population of the thermally coupled energy levels follows the Boltzmann distribution and the FIR of two emissions can be written as follows [34-35]:

$$R = \frac{I_H}{I_S} = \frac{N(^2H_{11/2})}{N(^4S_{3/2})} = \frac{g_H \sigma_H \omega_H}{g_S \sigma_S \omega_S} \exp(\frac{-\Delta E}{KT}) = C \exp(\frac{-\Delta E}{KT}) \quad (3)$$

Where I_H and I_S are *intensities* (*the integrated areas* below the emission curves) for the upper ($^2H_{11/2} \rightarrow {}^4I_{15/2}$) and lower ($^4S_{3/2} \rightarrow {}^4I_{15/2}$) thermally coupled levels transitions, respectively. N, g, σ, ω are the number of ions, the degeneracy, the emission cross-section, the angular frequency of fluorescence transitions from the $^2H_{11/2}$ and $^4S_{3/2}$ levels to the $^4I_{15/2}$ level, respectively. K is the Boltzmann constant, and ΔE is the energy gap between the $^2H_{11/2}$ and $^4S_{3/2}$ levels, T is absolute temperature and C is proportionality constant.

Figure 6a and b *present* the behaviors of FIR (I_H/I_S) for samples $NaYTiO_4$: $0.14Yb^{3+}$, $0.05Er^{3+}$ and $NaGdTiO_4$: $0.14Yb^{3+}$, $0.05Er^{3+}$ as a function of temperature, in which the fitting results analysized using *Eq.* (3) are also inclued. It is found that the monolog of experimental FIR data are fitted as a straight line on the inverse of temperature from Fig.6a. The solopes of two lines are about 1079 and 1069, and the energy gap ΔE could be calculated to about 783 and 765 cm^{-1} in $NaYTiO_4$ and $NaGdTiO_4$, which is close to previous results in the range of 750-800 cm^{-1} [36-37]. The *dependences* of FIR on temperature are showed in Fig.6b, the *values* of the coefficient C is about 8.55 and 8.85 by the best fit curves.

The sensor sensitivity is an important reference parameter, which is defined as the rate of the FIR (R) changes with temperature and expressed using the following formula [38]:

$$S = \frac{d(R)}{d(T)} = R\,(\frac{\Delta E}{KT^2}) \quad (4)$$

Fig.6c shows the sensitivity (S) as a function of absolute temperature. With the increase of temperature, the sensitivity of Er^{3+}-Yb^{3+} co-doped $NaYTiO_4$ reached the maximum about 0.0045 K^{-1} at 510 K, but the sensitivity for Er^{3+}-Yb^{3+} co-doped $NaGdTiO_4$ keep a constant after reach at maximum 0.0045 K^{-1} at temperature of 480 K. It indicates that Yb^{3+}/Er^{3+} ions co-doped $NaLnTiO_4$ (Ln=Y, Gd) phosphors could be used as potential candidates for optical temperature sensors based on the FIR technique.

4. Conclusions

The Yb^{3+}/Er^{3+} ions co-doped $NaLnTiO_4$ (Ln=Y, Gd) up-conversion (UC) phosphors were prepared by sol-gel method, and the optimal preparation parameters for $NaLnTiO_4$ (Ln=Y, Gd) were also determined as 0.05 Er^{3+}, 0.14 Yb^{3+} at 900 ℃. Under 980 nm excitation, samples emit orange light and their UC spectra are composed of prominent green emission centered at 530, 550 and red emission peaked at 668 nm originating from $^2H_{11/2} \rightarrow {}^4I_{15/2}$, $^4S_{3/2} \rightarrow {}^4I_{15/2}$ and $^4F_{9/2} \rightarrow {}^4I_{15/2}$ transitions of Er^{3+} ion, respectively. The lifetimes of green emission centered at 550 nm, possible UC processes and mechanism *investigations* indicate that emission *are* two-photon *processes* and the efficient energy transfer from Yb^{3+} to Er^{3+} plays an important role in UC process. The *dependences* of FIR for the samples $NaLnTiO_4$: 0.05 Er^{3+}, 0.14 Yb^{3+} (Ln=Y, Gd) with optimal compositions on temperature were measured in the range of 300-510 K, and the *sensitivities* of samples reach the same maximum 0.0045 K^{-1} for $NaYTiO_4Er^{3+}$-Yb^{3+} at 510 K and $NaGdTiO_4$: Er^{3+}-Yb^{3+} at 480 K, respectively. The results illuminate that the present UC phosphors could be used as promising *candidates* for optical temperature sensors.

Acknowledgement

This work was supported by the high-level talent project of Northwest University, National Natural Science Foundation of China (No. 11274251,11274299, 11374291), Ph.D. Programs Foundation of Ministry of Education of China (20136101110017), Technology Foundation for Selected Overseas Chinese Scholar, Ministry of Personnel of China (excellent), Natural Science Foundation of Shaanxi Province (No.2014JM1004) and Foundation of Key Laboratory of Photoelectric Technology in Shaanxi Province (12JS094).

References

[1] Z. Boruc, M. Kaczkan, B. Fetlinski, S. Turczynski, M. Malinowski, Opt. Lett., 2012, **37**, 5214-5216.

[2] C. D. S. Brites, P. P. Lima, N. J. O. Silva, A. Millán, V. S. Amaral, F. Palacio, L. D. Carlos, Nanoscale, 2013, **5**, 7572-7580.

[3] C. D.S. Brites, P. P. Lima, N. J. O. Silva, A. Milla´n, V. S. Amaral, F. Palacio, L. D. Carlos, New. J. Chem., 2011, **35**, 1177-1183.

[4] S. Chattopadhyay, P. Sen, J. T. Andrews, P. K. Sen, J. Appl. Phys., 2012, **111**, 034310.

[5] F. Vetrone, R. Naccache, A. Zamarro´n, A. J. Fuente, F. Sanz-Rodrıguez, L. M. Maestro, E. M. Rodriguez, D. Jaque, J. G Sole´, J. A. Capobianco, ACS Nano, 2010, **4**, 3254-3258.

[6] J. M. Yang, H. Yang, L. Lin, ACS Nano, 2011, **5**, 5067-5071.

[7] C. D. S. Brites , P. P. Lima , N. J. O. Silva , A. Millán , V. S. Amaral, F Palacio, L. D. Carlos, Adv. Mater., 2010, **22**, 4499-4504.

[8] C. Joshia, A. Dwivedib, S. B. Rai, Spectrochim Acta A, 2014, **129**, 451-456.

[9] D. Li, Y. Wang, X. Zhang, K. Yang, L. Liu, Y. Song, Opt. Commun., 2012, **285**, 1925-1928.

[10] W. Xu, X. Gao, L. Zheng, Z. Zhang, W. Cao, Sens. Actuators B, 2012, **173**, 250-253.

[11] B. Dong, B. Cao, Y. He, Z. Liu, Z. Li, Z. Feng, Adv. Mater., 2012, **24**, 1987-1993.

[12] N. Rakov, G. S. Maciel, Opt. Lett., 2014, **39**, 3767-3769

[13] S. Zhou, K. Deng, X. Wei, G. Jiang, C. Duan, Y. Chen, M. Yin, Opt. Commun, 2013, **291**, 138-142.

[14] H. Zheng, B. Chen, H. Yu , J. Zhanga, J. Suna, X. Li, M. Sun, B. Tian, S. Fu, H. Zhong, B. Dong, R. Hua, H. Xi, J. Colloid Interface Sci., 2014, **420**, 27-34.

[15] M. Quintanilla, E. Cantelar, F. Cussó, M. Villegas, A. C. Caballero, Appl. Phys. Express, 2011, **4**, 022601.

[16] Y. Yang, C. Mi, F. Yu, X. Su, C. Guo, G. Li, J. Zhang, L. Liu, Y. Liu, X. Li, Ceram. Int., 2014, **40**, 9875-9880.

[17] N. Rakova, G. S. Maciel, Sens. Actuators B, 2012, **164**, 96-100.

[18] G. Blasse, A. Bril, J. Chem. Phys., 1968, **48**: 3652-3656

[19] A. E. Lavat, E. J. Baran, J. Alloy Compd., 2006, **419**: 334–336

[20] H. Zhong, X. Li, R. Shen, J. Zhang, J. Sun, H. Zhong, L. Cheng, Y. Tian, B. Chen, J. Alloy Compd., 2012, **517**, 170

[21] K. Toda, Y. Kameo, M. Ohta, M. Sato, J. Alloy Compd., 1995, **218**, 228-232

[22] N. Zhang, C. Guo, H. Jing, RSC advances 2013, **3**, 7495-7502

[23] N. Zhang, C. Guo, J. Zheng, X. Su, J. Zhao, J. Mater. Chem. C, 2014, **2**, 3988-3994

[24] Y. Jiang, R. Shen, X. Li, J. Zhang, H. Zhong,Y. Tian, J. Sun, L. Cheng, H. Zhong, B. Chen, Ceram. Int., 2012, **38**, 5045-5051.

[25] R. D. Shannon, Acta Cryst. 1976, **A32**, 751-767.

[26] J. Li, J. Sun, J. Liu, X. Li, J. Zhang, Y. Tian, S. Fu, L. Cheng, H. Zhong, H. Xia, B. Chen, Mater. Res. Bull., 2013, **48**, 2159-2165

[27] T. Li, C. Guo, Y. Wu, L. Li, J. H. Jeong, J. Alloy Compd., 2012, **540**, 107–112.

[28] I. Etchart , A. Huignard , M. Bérard, M. N. Nordin, I. Hernández, R. J. Curry, W. P. Gillin, A. K. Cheetham, J. Mater. Chem., 2010, **20**, 3989-3994.

[29] G. Chen, G. Somesfalean, Y. Liu, Z. Zhang, Q. Sun, F. Wang, Phys. Rev. B, 2007, **75**, 195204.

[30] T. Li, C. Guo, L. Li, Opt. Express, 2013, **21**, 18281-18289.

[31] J. C. Boyer, F. Vetrone, L. A. Cuccia, J. A. Capobianco, J. Am. Chem. Soc., 2006, **128**,7444-7445.

[32] H. Jing, C. Guo, G. Zhang, X. Su, Z. Yang, J. H. Jeong, J. Mater Chem, 2012, **22**, 13612-13618.

[33] T. Fujii, K. Kodaira, O. Kawauchi, N. T. H. Yamashita, MAnpo, J. Phys. Chem. B, 1997, **101**, 10631-10637.

[34] M. D. Shinn and W. A. Sibley, M. G. Drexhage, R. N. Brown, Phys. Rev. B, 1983, **27**, 6635–6648.

[35] L. Li, C. Guo, S. Jiang, D. K. Agrawal, T. Li, RSC Adv., 2014, **4**, 6391-6396.

[36] X. Wang, X. Kong, Y. Yu, Y. Sun, H. Zhang, J. Phys. Chem. C, 2007, **111**, 15119-15124.

[37] S. A. Wade, S. F. Collins, G. W. Baxter, J. Appl. Phys. 2003, **94**, 4743-4756.

[38] V. K Rai, A. Pandey, R. Dey, J. Appl. Phys., 2013, **113**, 083104.

Figure Captions

Figure 1 XRD patterns of $NaLnTiO_4$ (Ln = Y, Gd) phosphors: (a) $NaY_{1-x}Yb_xEr_yTiO_4$ phosphors and (b) $NaGd_{0.81}Yb_{0.14}Er_{0.05}TiO_4$ phosphors annealed at 900 ℃ for 2 h in air.

Figure 2 UC luminescence spectra of $NaY_{1-x-y}Yb_xEr_yTiO_4$: xYb^{3+}, yEr^{3+} (a) x=0.10; y=0.01, 0.03, 0.05, 0.07, 0.09 and (b) y=0.05; x=0, 0.06, 0.08, 0.10, 0.12, 0.14, 0.16, 0.18, 0.20 under excitation at 980 nm.

Figure 3 (a) Energy level diagram of the Yb^{3+}, Er^{3+} ions and the proposed UC mechanisms in Er^{3+}/Yb^{3+} co-doped $NaYTiO_4$ under 980 nm excitation; (b) and (c) Dependence of UC luminescence intensity of $NaY_{0.81}Yb_{.0.14}Er_{0.05}TiO_4$ and $NaGd_{0.81}Yb_{.0.14}Er_{0.05}TiO_4$ upon the pumping power, respectively.

Figure 4 The temporal evolution of the green ${}^4S_{3/2}\rightarrow{}^4I_{15/2}$ emissions in $NaY_{0.95-x}Yb_xEr_{0.05}TiO_4$: $0.05Er^{3+}$, xYb^{3+} (x=0, 0.08).

Figure 5 Temperature dependence of the green UC luminescence spectra of $NaYTiO_4$: $0.14Yb^{3+}$, $0.05Er^{3+}$ (a) and $NaGdTiO_4$: $0.14Yb^{3+}$, $0.05Er^{3+}$ (b) under 980 nm excitation (The spectra are normalized to the most intense emission peak at about 551 nm).

Figure 6 Temperature depentent FIR (a), (b) and relative sensitivities (c) for $NaYTiO_4$: Er^{3+}/Yb^{3+} (left column) and $NaGdTiO_4$: Er^{3+}/Yb^{3+} (right column) phosphors.

Figures

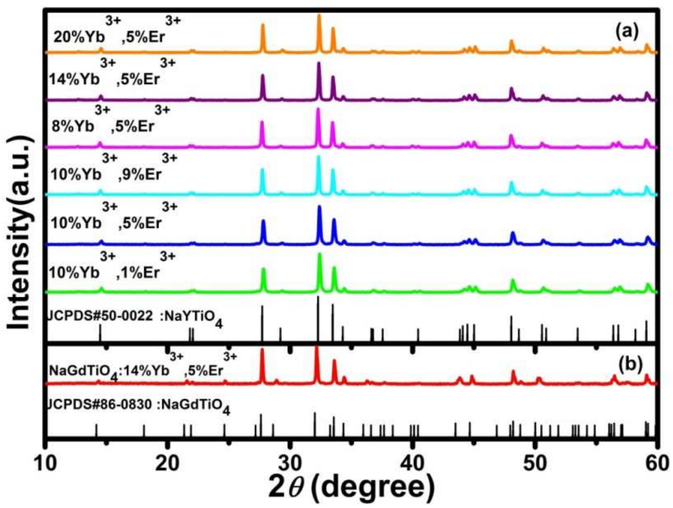

Fig. 1 XRD patterns of $NaLnTiO_4$ (Ln = Y, Gd) phosphors: (a) $NaY_{1-x}Yb_xEr_yTiO_4$ phosphors and (b) $NaGd_{0.81}Yb_{0.14}Er_{0.05}TiO_4$ phosphors annealed at 900 ℃ for 2 h in air.

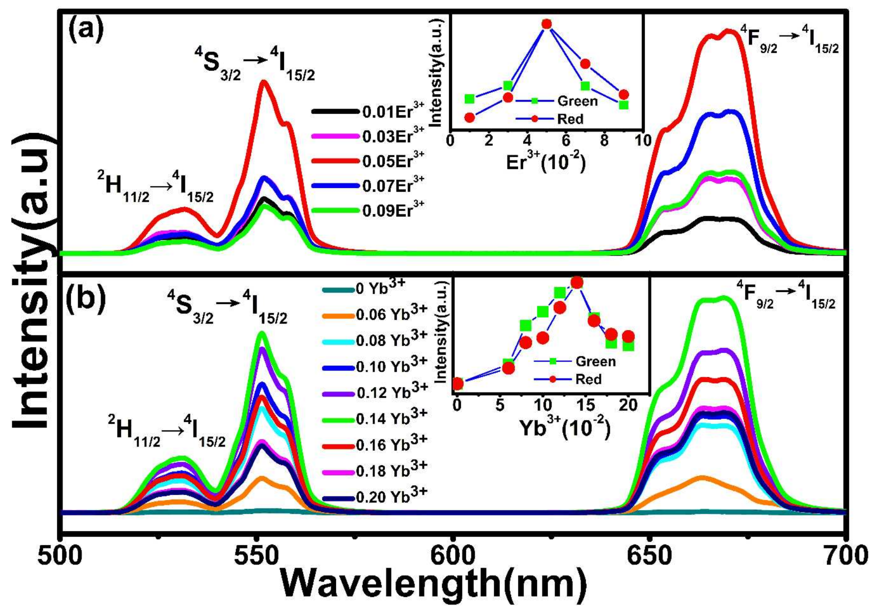

Fig. 2 UC luminescence spectra of $NaY_{1-x-y}Yb_xEr_yTiO_4$: $x$$Yb^{3+}$, $y$$Er^{3+}$ (a) x=0.10; y=0.01, 0.03, 0.05, 0.07, 0.09 and (b) y=0.05; x=0, 0.06, 0.08, 0.10, 0.12, 0.14, 0.16, 0.18, 0.20 under excitation at 980 nm.

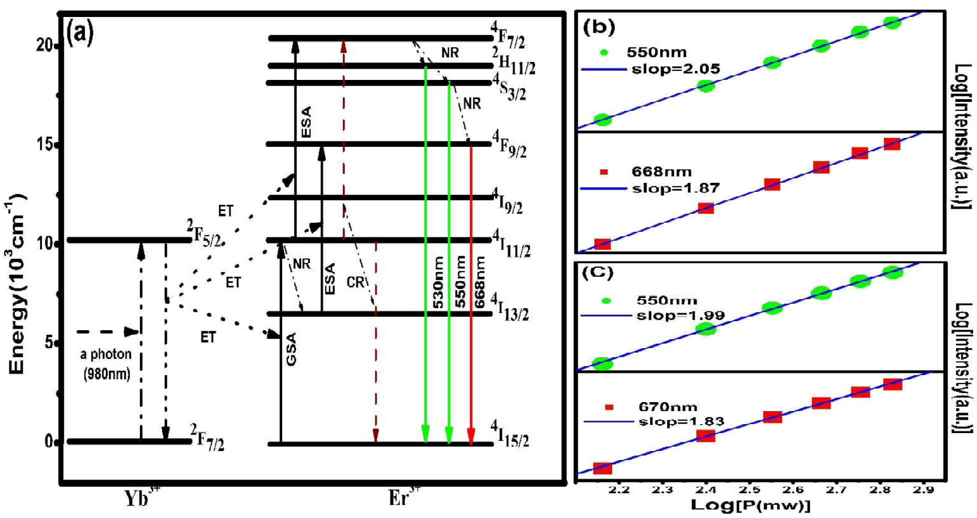

Fig. 3 (a) Energy level diagram of the Yb^{3+}, Er^{3+} ions and the proposed UC mechanisms in Er^{3+}/Yb^{3+} co-doped $NaYTiO_4$ under 980 nm excitation; (b) and (c) Dependence of UC luminescence intensity of $NaY_{0.81}Yb_{.0.14}Er_{0.05}TiO_4$ and $NaGd_{0.81}Yb_{.0.14}Er_{0.05}TiO_4$ upon the pumping power, respectively.

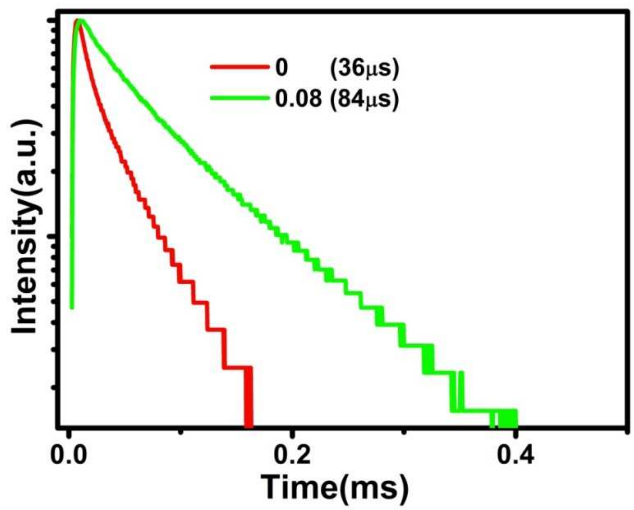

Fig. 4 The temporal evolution of the green $^4S_{3/2}\rightarrow{}^4I_{15/2}$ emissions in $NaY_{0.95-x}Yb_xEr_{0.05}TiO_4$: $0.05Er^{3+}$, xYb^{3+} (x=0, 0.08).

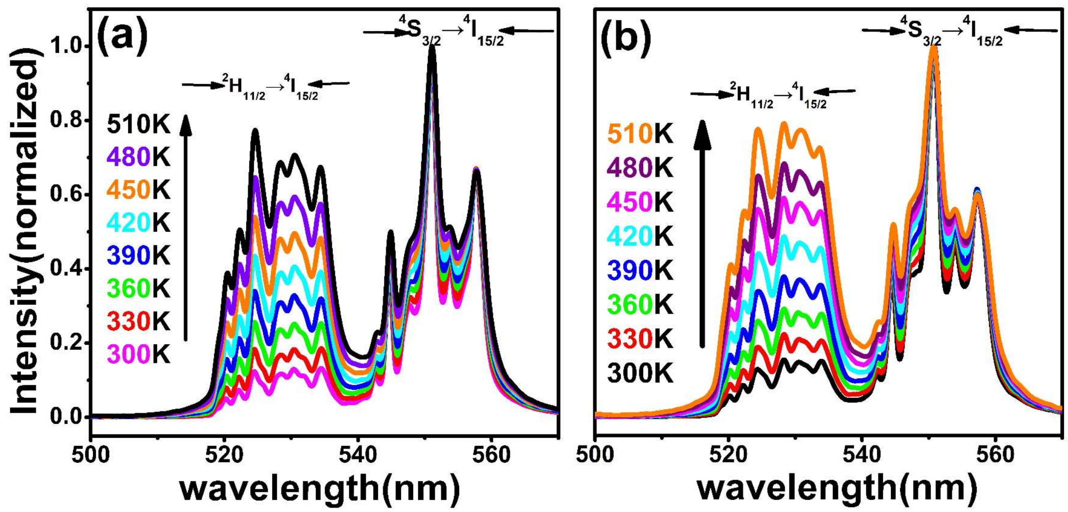

Fig.5 Temperature dependence of the green UC luminescence spectra of $NaYTiO_4$: $0.14Yb^{3+}$, $0.05Er^{3+}$ (a) and $NaGdTiO_4$: $0.14Yb^{3+}$, $0.05Er^{3+}$ (b) under 980 nm excitation (The spectra are normalized to the most intense emission peak at about 551 nm).

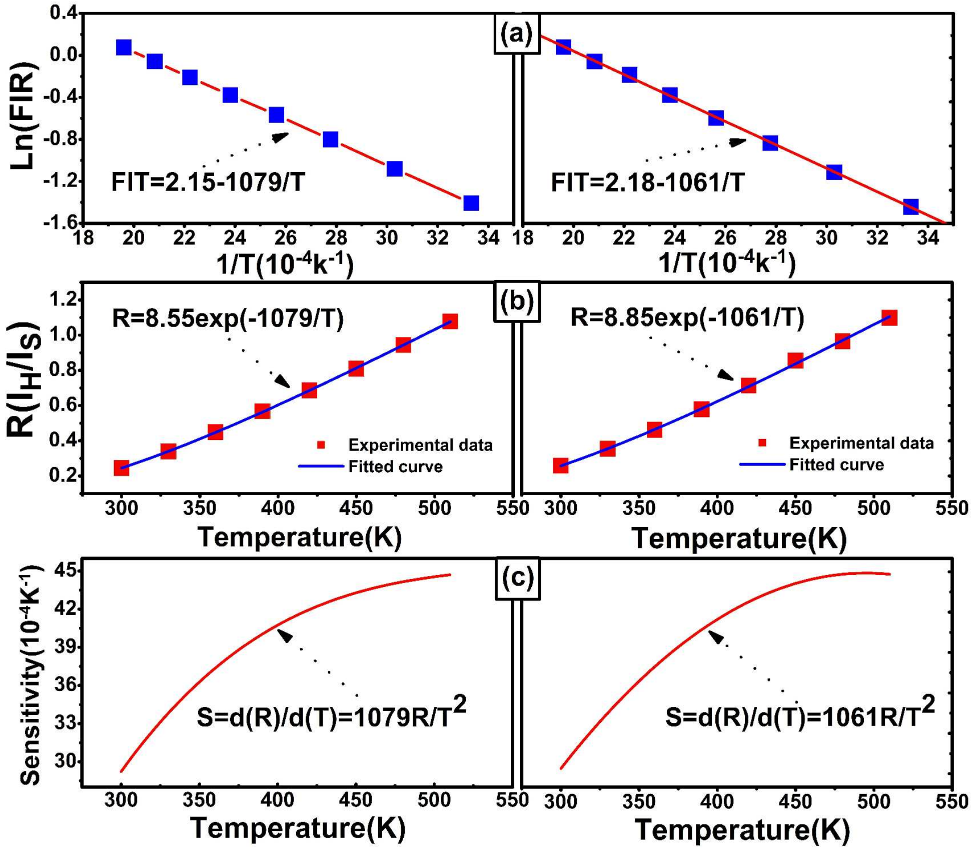

Fig. 6 Temperature depentent FIR (a), (b) and relative sensitivities (c) for $NaYTiO_4$: Er^{3+}/Yb^{3+} (left column) and $NaGdTiO_4$: Er^{3+}/Yb^{3+} (right column) phosphors.